INSTITUTE OF PLASMA PHYSICS

NAGOYA UNIVERSITY

Characteristics of Hot Electron Ring in a Simple Magnetic Mirror Field

M. Hosokawa and H. Ikegami

(Received - Nov. 27, 1980)

IPPJ- 497 December 1980

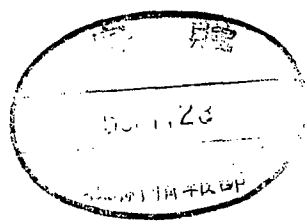

RESEARCH REPORT

NAGOYA, JAPAN

Characteristics of Hot Electron Ring in a Simple Magnetic Mirror Field

M. Hosokawa and H. Ikegami

(Received - Nov. 27, 1980)

IPPJ- 497 December 1980

Further communication about this report is to be sent to the Research Information Center, Institute of Plasma Physics, Nagoya University, Nagoya 464, Japan

---

*Paper presented at the Workshop on EBT Ring Physics, Oak Ridge, Tennessee, U.S.A., December 3-5, 1979.

ABSTRACT

Characteristics of hot electron ring are studied in a simple magnetic mirror machine (mirror ratio 2:1) with a diameter of 30 cm at the midplane and with the distance of 80 cm between the mirrors. Maximum microwave input power is 5 kW at 6.4 GHz with the corresponding power density of approximately 0.3 W/cm^3.

With a background cold plasma of 4×10^{11} cm^{-3}, hot electron rings are most effectively generated in two cases when the magnetic field on the axis of the midplane is set near the fundamental or the second harmonic electron cyclotron resonance to the applied microwave frequency. Density profile of the hot electrons is observed to take a so-called ring shape with a radius controllable by the magnetic field intensity and with an axial length of approximately 10 cm. The radial cut view of the ring, however, indicates an M shape density profile, and the density of the hot electrons on the axis is about one half of the density at the ring. Approximately 30 msec is needed before generating the hot electron ring at the density of 10^{10} cm^{-3} with an average kinetic energy of 100 keV. The ultimate energy distribution function is observed to have a stepwise cut in the high energy tail and no energetic components above 1 MeV are detected.

The hot electron ring is susceptible to a few instabilities which can be artificially triggered. One of the instabilities is observed to associate with a loss of lower energetic electrons and microwave bursts. At the instability, the ring shape is observed to transform into a filled cylinder in a few microseconds and disappear.

Characteristics of Hot Electron Ring in a Simple Magnetic Mirror Field

M. Hosokawa and H. Ikegami
Institute of Plasma Physics, Nagoya University,
Nagoya 464, Japan

1. INTRODUCTION

It has been known for a long time that the hot electron plasma generated by microwaves in a magnetic mirror configuration takes a ring shape.[1,2]

Because of high beta property of the hot electron ring, its application to magnetic fusion devices has attracted great interests. For example, poloidal Heliotron ring or Dawson ring could be replaced by the hot electron ring which has no support losses nor anomalous scattering at the stagnation points. Since the stabilization effect due to minimum average B with the use of poloidal ring currents has been well studied experimentally,[3-5] the stabilization and physics of the hot electron ring is subject to further investigation.

In the bumpy torus concept where hot electron rings play a crucial role for stabilization,[6-8] the behavior of the hot electron ring is anticipated to have a great similarity to that in a simple mirror.[9-12]

In the following section, general description is given to microwave generated plasmas in a simple magnetic mirror machine, TPM, at the Institute of Plasma Physics, Nagoya University. Spatial structure or the density profile of the hot electron ring is discussed in section 3. Experimental studies on the evolution of energy distribution function of the hot electrons are made in section 4. In the last section, several instabilities are investigated by triggering them artificially with their effects on the density profile and energy distribution of the hot electrons.

2. GENERAL DESCRIPTION OF THE TPM MIRROR MACHINE

The hot electron ring was generated by the microwave discharge in a

simple mirror field with a mirror ratio R = 3.4 by means of the electron cyclotron heating and is contained in a cylindrical cavity 40 cm long and 30 cm in diameter. The discharge is produced by a microwave pulse at 6.4 GHz with 20 msec duration and powers variable up to 5 kW. The microwave power is introduced radially through two opposite pairs of waveguide ports in the cavity wall. The schematic diagram of the device is shown in Fig.1.

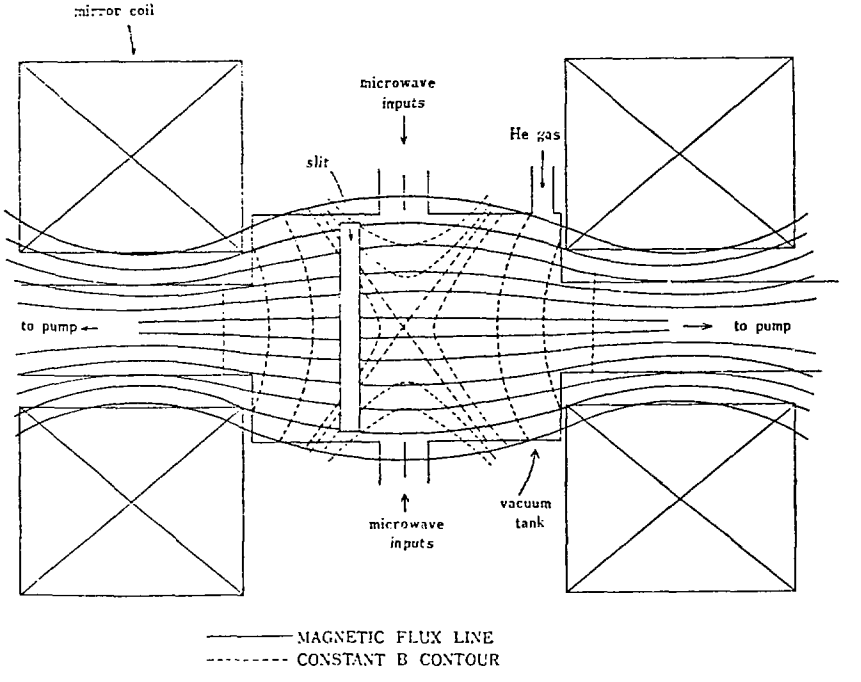

Fig.1. Schematic diagram of TPM machine. The bold hyperbola-like lines across the flux lines indicate the fundamental cyclotron resonance region.

The plasma produced at various power levels are very similar both in the electron temperature and the electron density. For the most part, the microwave was pulsed and helium afterglow plasma was studied.

In summary, various diagnostic techniques revealed the following properties of the plasma in TPM mirror machine:

i) the plasma consists of three components: hot electrons, cold electrons and helium ions;

ii) plasma density is composed of about 10^9-10^{10} hot electrons/cm^3 and 10^{11}-10^{12} cold electrons/cm^3;

iii) the average energy is typically 100 keV for hot electrons and approximately 20 eV for the cold electrons;

iv) temperature of ions is about 7-10 eV;

v) the hot electrons take a density profile of shell structure with 10 cm diameter;

vi) plasma density decay time is about several tens of msec, which does not depend on the heating microwave power.

3. STRUCTURE OF HOT ELECTRON RING[1]

In order to determine the density and temperature of the hot electrons, X-ray photons are taken through a 0.1 mm-thick Mylar window onto a 3" dia. x 3" long NaI scintillator being collimated by an X-ray telescope. The solid angle subtended by the crystal through the collimator is about 10^{-5} sr and it collects photons from a cylindrical volume of plasma approximately 10 cm long with a cross section of 2 cm^2. The collimation system excludes any reception from the chamber walls. When the X-ray telescope is moved along the vertical slit (see Fig.1), it is possible to calculate the radial distribution of X-ray emission by using Abel's transformation. This distribution is directly proportional to that of the hot electron density. The hot electrons are thus observed to be bunched in a shell structure throughout the microwave discharge and the afterglow of the plasma as shown in Fig.2. The radial density distribution of the cold electrons has the shape of a bell centered on the axis of the machine, while after the power has been removed, the top of the bell is depleted to form a shell. The fact assures that the cold electrons present in the plasma during the afterglow are those produced by ionization of neutral atoms by the hot electrons present

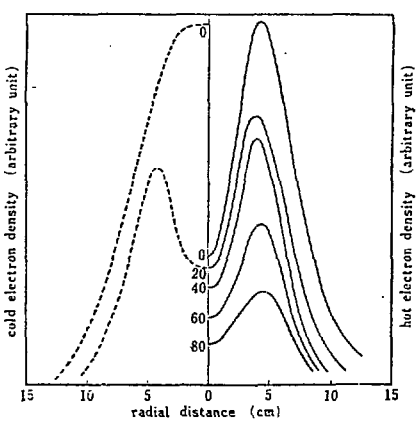

Fig.2. Plot of the radial density distribution of the electrons, after Abel's transformation. The dashed curves in the left half are related to the cold electrons and solid curves in the right half to the hot electrons. Parameters are the times (msec) after the front of the heating microwave pulse, of 20-msec duration. Each observation is made for 20 msec.

in the shell. The decay of this new cold electron distribution is determined now by the longer lifetime (30-100 msec) of the hot electrons.

It has been confirmed[1,6,16] that the location of the hot-electron shell corresponds to the throat of the single-lobe hyperboloidlike surface of constant magnetic field intensity, which provides the second harmonic resonance for the heating microwave at 6.4 GHz. As the magnetic field increases, the radius of the throat increases and the radius of the hot-electron shell is observed to follow this growth. In other words, the hot-electrons are generated within the mirror always at the zone of constant magnetic field intensity which provides the electron cyclotron frequency at 3.2 GHz.

Structure of the hot electron ring along the magnetic lines of force is studied by measuring the perturbed magnetic field intensity due to the presence of the hot electron ring. A Hall element is fit at the tip of stainless steel pipe which is movable along the axial magnetic lines of force without much perturbation on the hot electrons. The results are shown in Fig.3, where paramagnetic perturbation is observed over 10 cm at the midplane when the hot electron ring is established after 10 msec of heating. Away from the ring, the perturbation is observed to be diamagnetic.

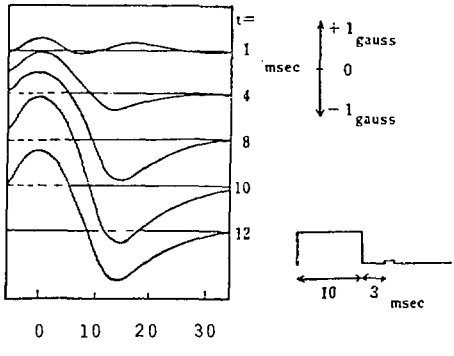

Fig.3. Perturbation of axial magnetic field on the axis with a time of heating as a parameter.

The structure of the hot electron plasma is thus observed to be a tubing of approximately 10 cm in diameter and 10 cm in length rather than a thin ring. The location is determined by the constant $|B|$ surface in the midplane that satisfies the second cyclotron harmonic resonance to the applied microwave frequency. The length is obviously a function of pitch angles, so that it will strongly depends on the field shape as well as the microwave power density.

One may be interested in production of hot electrons at the fundamental

cyclotron resonance.[8] The ratio of the heating rate due to the second harmonic resonance, Γ_2, to that for the fundamental resonance, Γ_1, may be given by

$$\frac{\Gamma_2}{\Gamma_1} \sim \frac{J_2^2(k\rho)}{J_1^2(k\rho)} \quad ,$$

where k is the wavenumber and ρ is the Larmor radius of the electron. The condition, $\Gamma_2/\Gamma_1 > 1$, requires $k\rho \gtrsim 1.5$, which is satisfied for the electron with the energy greater than 200 keV under the experimental condition: B = 1150 G and k = 1.28 cm^{-1}. The main reason why the second harmonic resonance is so effective in generating the hot electrons is due to the fact that in the present mirror field the electrons trapped in the midplane with large pitch angles turn out to that they can gain energy only at the second harmonic resonance.

4. ENERGY DISTRIBUTION OF HOT ELECTRONS[15]

Spectral distribution of the X-ray bremsstrahlung is normally used to determine the hot electron temperature, for which a typical spectral distribution is shown in Fig.4. If we assume the hot electrons to have the Maxwellian energy distribution and adopt the quasi-classical approximation (Weiche-Näherrung formula) for the total cross-section for the emission of a photon with energy k, the photon number $n(k)$ within the energy interval $(k, k + \Delta k)$ is given by

$$n(k) = 3.38 \times 10^{-15} Z^2 N n T^{-1/2} k^{-1} \exp(-k/T) \qquad (1)$$

(photons/sec·cm^3keV)

where N is the density of atoms with the atomic number Z, n is the hot-electron density, and T is the hot-electron temperature in keV. The electron temperature can be roughly estimated from the slope of log $kn(k)$ vs. k. However, the quasi-classical approximation is valid only under the condition $2\pi Ze^2/hv \gg 1$, to which the corresponding critical energy of the electron in hydrogen atoms is as low as 700 eV. For the hot electron plasma in the present experiment, Born's approximation is preferable, whose applicability is based on the condition $2\pi Ze^2/hv \ll 1$. With the Born approximation, we get

$$\eta(k) = 1.69 \times 10^{-15} Z^2 N n T^{-1/2} k^{-1} \exp(-k/2T) K_0(k/2T) \qquad (2)$$

(photons/sec·cm^{3}keV)

where $K_0(Z)$ is the modified Bessel function.

From the energy spectrum $\eta(k)$ obtained with the use of a NaI(Tℓ) scintillator. The energy distribution function of the hot electrons is calculated from the Volterra's integral equation given by

$$\eta(k) = \frac{16}{3} \phi \mu N k^{-1} \int_k^\infty \sqrt{2E/m}\, G(E, k) E^{-1} f(E) dE \qquad (3)$$

where $\phi = Z^2 r_0^2/137$, $\mu = mc^2$, $f(E)$ is the energy distribution function of the electron, and

$$G(E, k) = \ln\{(\sqrt{E} + \sqrt{E - k})^2/k\} \qquad (4)$$

is the energy dependent part of the total cross-section for the bremsstrahlung of photon with energy k by the electron with energy E. If f(E) is assumed to be Maxwellian, Eq.(3) is reduced to Eq.(2).

In order to find f(E) from the raw data as shown in Fig.4 with the use of Eq.(3), it is necessary to smooth the scattered distribution of $\eta(k)$ vs. k, which is obtained in a punched, paper tape from a pulse height analyzer. Then, those measured points ($\eta(k)$, k) are simulated by an elastic string where each point is connected by a proper spring. Fairing is carried out by using a computer in such a way that the elastic energy of the system becomes minimum. Let assume a smooth, elastic string $g(k_i)$ which has flexure rigidity EI, and a spring constant K, then the elastic energy of the system is given by

$$U = \frac{1}{2} K \sum_i \{g(k_i) - \eta(k_i)\}^2 + \frac{1}{2} EI \sum_i g''(k_i)^2 \qquad (5)$$

A smooth curve g(k) which best represents the measured points is determined by an elastic string resulting in the minimum value of U. Such a fairing technique may more or less depend upon the subjective expectation of those who engage in the problem, and arbitrariness could be introduced through the determination of K and EI. An example of the energy distribution function determined from Eq.(3) after the fairing process described above is

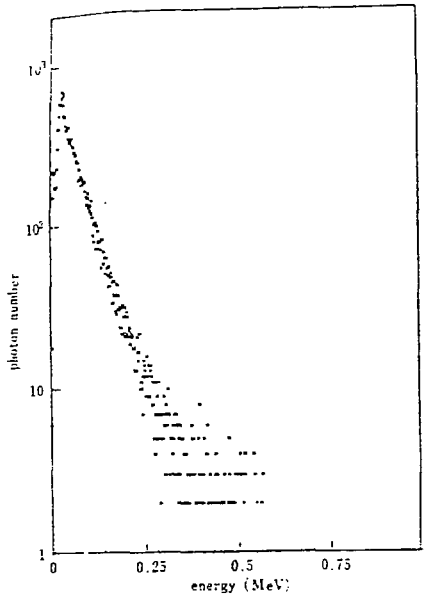

Fig.4. Typical energy spectrum of the X-ray bremsstrahlung. The ordinate is the photon number obtained with the use of a 400-channel pulse-height analyzer.

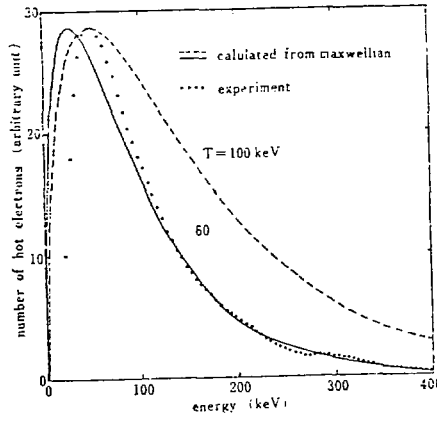

Fig.5. Energy distribution function of the hot electron calculated from the raw data in Fig.4.

shown in Fig.5, for which the raw data shown in Fig.4 is examined.

The energy distribution resembles a Maxwellian distribution with the temperature 60 keV, but its peak does not locate at 30 keV, but at 50 keV. One may find that the calculated distribution function reflects the feature of a loss-cone distribution, except a slight bump in the high energy tail.

Energy distribution determined from the X-ray spectrum tends to smooth bumps and hollows. Direct measurements of the distribution functions with the use of a solid state detector are made simultaneously. The detector is located in the mirror end by 70 cm behind the mirror point, and in order to protect the detector from bombardment and burning by a copious amount of hot-electrons, the detector is mounted behind a 1 mm-thick lead disk with a hole of 0.1 mm in diameter. Therefore, the solid state detector accepts the hot electrons being lost into the loss cone, and for those electrons to reach onto the detector, their pitch angle in terms of $v_\perp/v_\parallel$ must be at least smaller than 0.1 at the point of detection. However, this does not bring about any serious modification of the energy distribution function, since the detector is located outside the mirror trap on the longitudinal axis of the magnetic field.

Some examples of thus measured energy distribution functions are shown

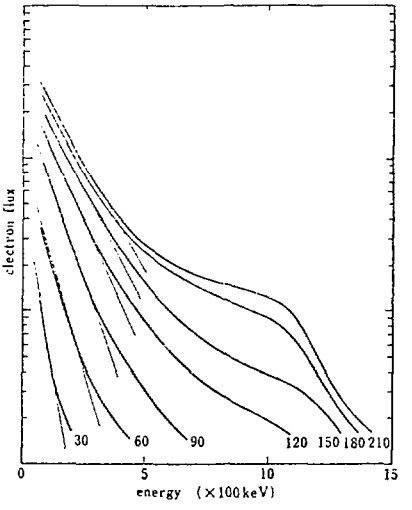

Fig.6. Electron energy bistribution measured by silicon surface barrier detectors. The ordinate is the electron flux in logarithmic scale. Input microwave pulse is of 200-msec duration at the peak power 4 kW. Gas is helium at 10^{-5} torr.

in Fig.6 where the energy distribution is measured for each successive 30 msec during the heating period of 200 msec. For the first 90 msec from the introduction of the microwave power, the so-called hot-electron temperature determined from the slope increases and thereafter tends to saturate. However, the average kinetic energy keeps on increasing by producing a plateau in the high energy tail of the distribution. Two reasons may account for the formation of the plateau in the high energy tail of the hot-electron energy distribution function. One is attributed to the fact that in a mirror trap, lower energy electrons are rapidly lost into the loss cone by the Coulomb scattering and that the ultimate kinetic energy of the electron is proportional to the lifetime in the stochastic heating process. High energy electrons are not only contained for a longer time in the mirror trap, but also they experience more heating because of that prolonged lifetime. The other reason is the experimental fact, which will be shown later, that higher energy electrons are stable against the whistler instability, which is the most dangerous among many coexisting instabilities in hot electron plasmas.

5. INSTABILITY OF HOT ELECTRON RING[13,14]

Electromagnetic triggering

In the present device, instabilities can be triggered by introducing an additional small microwave pulse of about 100 W at the same frequency as the heating microwave pulse after 1-50 msec from the end of the main pulse. For some conditions at pressures lower than the critical value of 10^{-4} torr, the plasma is spontaneously unstable. However, no physical difference is observed between the triggered instability and the spontaneous ones. When

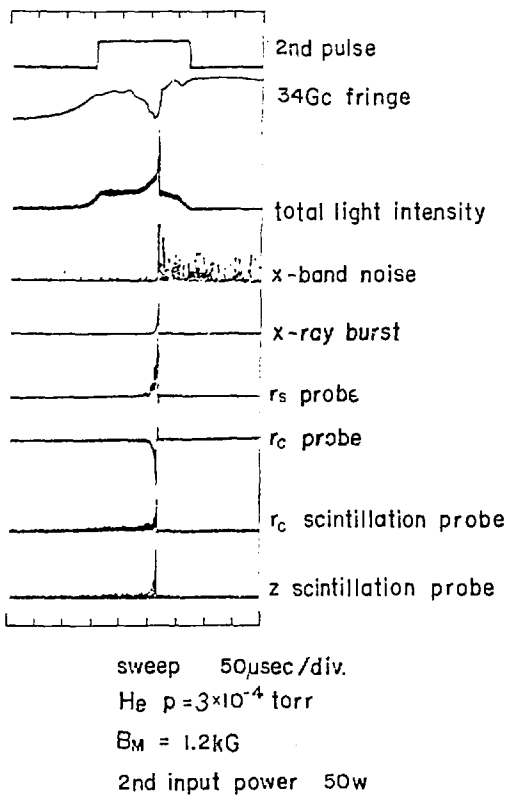

Fig.7. Signals accompanied with the instability triggered by the second microwave pulse (500 W). The onset of the instability is seen about 70 μsec after the pulse front. Helium (2×10^{-4} torr) is admitted in steady flow operation. In the 6th and 7th traces, r_s denotes a radially inserted Langmuir probe situated close to one end-walls of the cavity and r_c that at the center of the cylindrical cavity wall. Both probes are 10 cm apart on the same magnetic lines of force.

the pressure is above 8×10^{-4}, no instability could be triggered.

Some details of the triggered instability are shown in Fig.7. The instability is characterized by the sudden loss of hot electrons from the mirror bottle, but not of the cold electrons, and by the strong burst of microwave emission. The signals related to the hot electrons, like X-ray signal, microwave noise, scintillator output and diamagnetic signals, disappear within several microseconds. However, those related to the cold electrons, like Langmuir probe signal, light intensity and plasma density, decay at a slower time constant of about 200 μsec.

The strong microwave burst accompanied by the instability characterizes the nature of the instability. The microwave emission is composed of harmonics of 2.1 GHz for the typical mirror field (4000 G - 1200 G - 4000 G). Signals in the frequency range of 2.1, 4.2 and 6.3 GHz are collected by a loop antenna, while the higher-frequency emission (8.4, 10.5, 12.6 and the frequency region up to 18.9 GHz) are collected by X-band waveguides.

Although the magnetic field is varied around the optimum field intensity (4000 G - 1200 G - 4000 G), the variation of the microwave frequency (2.1 GHz) with the magnetic field at the mirror center is insensitive. This is quite reasonable, since the hot electrons are produced in a shell which touches the throat of the singlelobe hyperboloid-like surface of the constant magnetic field intensity, which provide the electron cyclotron frequency at 3.2 GHz. Since the frequency 6.4 GHz of the heating microwaves is fixed, the magnetic field intensity which give rise to the second harmonic resonance is also fixed. This fact implies that most hot electrons stay always around the region of 1140 gauss, corresponding to the second harmonic resonance, as far as the mirror remains around the optimum field intensity. When the field is changed drastically to give the production and heating at the center of the mirror at the fundamental cyclotron resonance, the frequency of the microwave radiation is doubled and becomes 4.2 GHz. The main contribution to the total power emission comes from the fundamental component and the power collected by the probe is found to be several 10 W within a bandwidth of 5 MHz. The amplitude of the burst increases with the growth rate of about 0.1 μsec, and reaches its maximum at about 1 μsec after the initiation of the instability.

Furthermore the radiation is detected by using a pair of two loop antennas inserted into the cavity each through the opposite end arms, one being fixed and the other movable along the axis of the machine. The microwave emission accompanied with the instability is found to be standing electromagnetic waves with the wavelength of 19 cm for 2.1 GHz. The mode of the wave is likely to be determined by the diameter of the cylindrical side arms of the vacuum chamber as a circular waveguide with TE_{11} mode. It will be also interesting to note that the instability destroys the hollow structure of the hot electron plasma. Experimental detection with the use of a Hall element is shown in Fig.8, where longitudinal magnetic perturbations are compared in two cases of stable and unstable decay. In case of unstable decay, either the hot electrons fill the hole, or the peaked edge disappears.

At the onset of the instability, the burst of end loss electrons, which escaped out of the magnetic mirror, was led onto an aluminum foil of six different thickness. The energetic electrons having passed through the foil impinge onto a plastic scintillator mounted on a photomultiplier. The resulting signal of the photon pulse-height is a function of the absorber

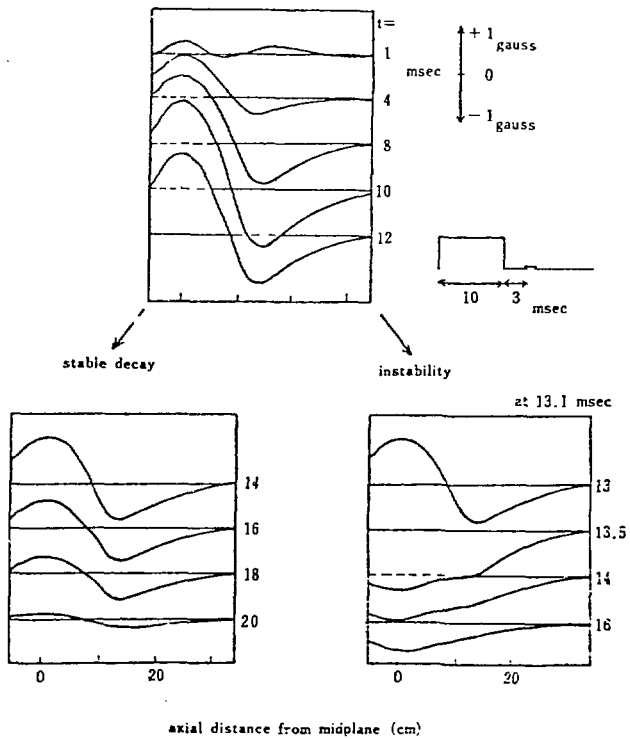

Fig.8. Plasma magnetic field along the axis of the machine. The parameters are the time in msec from the heating pulse front. When the instability is triggered at 13 msec, the anti-diamagnetic field disappears and larger diamagnetic fields are observed, which tells us that the shell structure has been carried away by the instability.

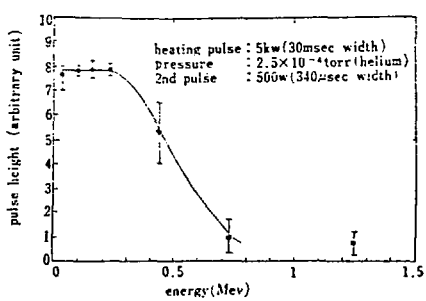

Fig. 9. Number of electrons escaped from the mirrors at the triggered instability, vs. their energy measured by the scintillator probe on the z-axis. The 2nd microwave pulse was applied 20 msec after the main pulse turnoff.

thickness. The pulse height spectrum in the presence of instability is shown in Fig.9, where the thickness has been related to the energy of the electrons from the range-energy curve. The electrons that escaped from the mirror during the quiet decay is observed to have a Boltzmann distribution with the temperature of about 150 keV.

Spontaneous instability

Transient state just after the removal of the microwave power have been observed to support various kinds of instability: interchange modes in simple mirror traps, electrostatic velocity space mode, and electromagnetic, whistler mode. During the heating period with the microwave power input, the stability aspect of the plasma is similar to that during the transient state, and the life time of the hot electron is supposed to be much shorter than it is during the stable, late afterglow. The fact is not only attributed to those instabilities, but also to the stochastic heating process itself in the sense that the diffusion in velocity space inevitably accompanies that in the coodinate space. During the heating period, a copious amount of X-ray emission is detected, which is obviously radiated by numbers of hot electrons colliding with the cylindrical wall of the vacuum chamber.

Spontaneous instabilities are typical of the hot electron plasma especially operated in a lower pressure regime. Effect of the instabilities on the energy distribution of the hot electrons are shown in Fig.10, where striking feature lies in the repetitive sudden decrease in the number of low energy electrons. These wild fluctuations are observed to correspond with spontaneous instabilities appearing regularly during the heating period. These instabilities have been studied in detail and identified to be the whistler instability. Driving whistler waves, resonant electrons consume their energy component perpendicular to the magnetic field and fall into the loss cone. From Fig.10 we see that those resonant electrons have energy below or approximately 50 keV. More important fact is that the electrons with higher energy are found not to participate with the instabilities. The fact implies that the cloud of high energy electrons be stable against the whistler instability, which is the most dangerous, absolute instability among many coexisting electrostatic and electromagnetic instabilities. This character will be in the favor of producing self-minimum B configuration with the use

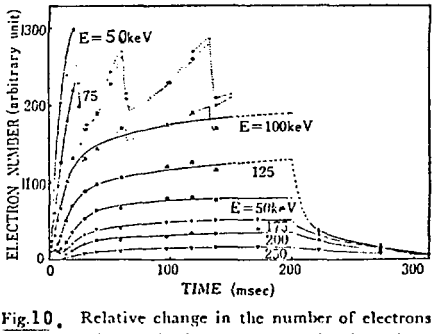

Fig.10. Relative change in the number of electrons with specified energy E. The heating microwave pulse is turned off at 200 msec.

of a collection of high energy electrons.

Electrostatic triggering[17]

The reason why the hot electron plasmas are stable against flute instabilities during afterglow, especially, is understood as being due to the presence of the cold electrons; the stabilization is attributed to a linetying effect caused by 'volume' short-circuiting cold electrons, which are continuously generated by the hot electrons ionizing residual helium atoms during the late afterglow plasma.

By controlling the cold electrons, one can artificially trigger hydrodynamical instabilities, as well as microscopic ones.

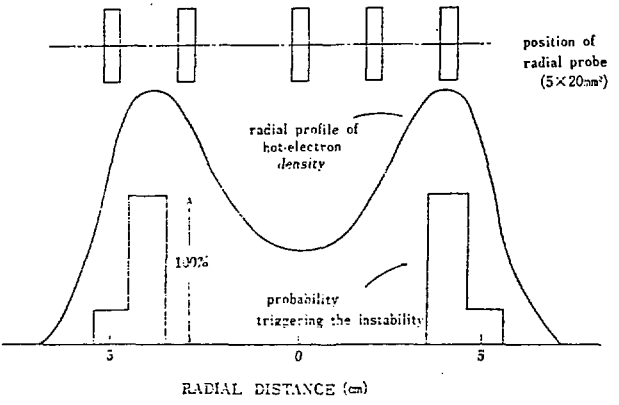

Fig.11. Probability of triggering the instability by radial probes ($P_1 \sim P_5$); probes P_4 and P_5 can trigger the instability.

In order to check the stabilization mechanism in detail, a disturbance is introduced by extracting the cold-electron component from the plasma by means of a pulsed Langmuir probe. Several probes are located at different radial positions and a pulse of positive voltage is applied to them against the plasma. As shown in Fig.11, probability of triggering instabilities are observed to be maximum when the positive voltage is applied to the end probe, located on the magnetic lines of force which pass through the region of maximum hot-electron density. It is important to recollect that the hot electrons take a ring shape, which is a peculiar feature of ECH hot electrons in a magnetic mirror trap. By varying the height and width of the pulse applied to the probe, the triggering probability is plotted as a function of the cold-electron number deprived by the pulsed Langmuir probe. As shown in Fig.12 the minimum number of electrons extracted to provoke the instability at 100 % is estimated to be 10^{12}, which corresponds to average 5 % depletion of local electron densities. Being associated with the extraction, a whistler instability is detected, as well as a flute-like, low frequency instability.

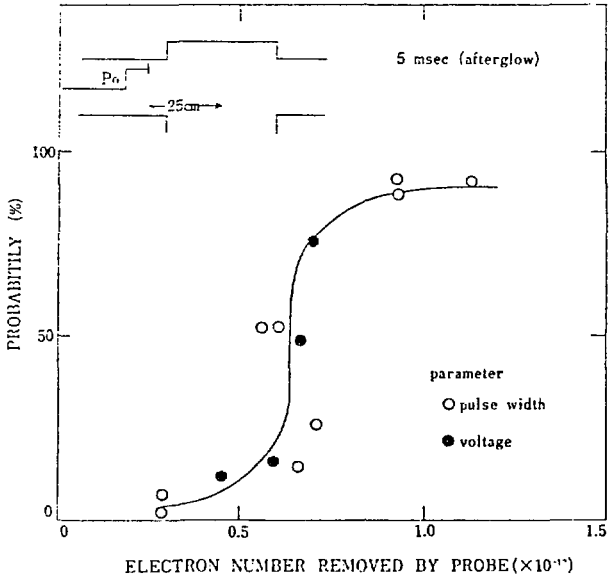

Fig.12. Probability of triggering instabilities by the probe P_o. Extracted electron number was estimated by time integration of the probe current.

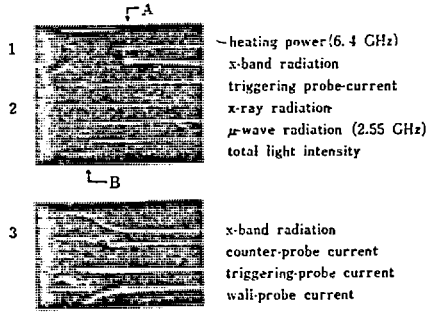

1 : 5 ms/div ; 2 : A expanded to 0.2ms/div
3 : B expanded to 20 μs/div

Fig.13. Instability is triggered in 3.5 msec after the heating power turned off.

The detailed process of the triggering is shown in Fig.13. About 8 μsec after the pulse current of cold-electron evulsion, flute-like instability, propagating azimuthally in the diamagnetic direction, is observed to grow and successively a whistler instability is detected in the similar way as described in the previous section of electromagnetic triggering.

In the present ECH plasma, the hot-electron energy is so high that the electromagnetic instability can easily compete with electrostatic ones. It should be noticed that hot electron plasmas are almost always electromagnetically unstable, since the condition $T_\perp/T_\parallel > 1$ is inevitable.

Experimentally a critical ambient, neutral gas pressure is observed below which the hot electron plasma carries various instabilities. The pressure is higher for higher microwave input power. The stable and unstable boundary with the input power of 5 kW is shown in Fig.14, where the quasi-stable region is determined by the electrostatic triggering.

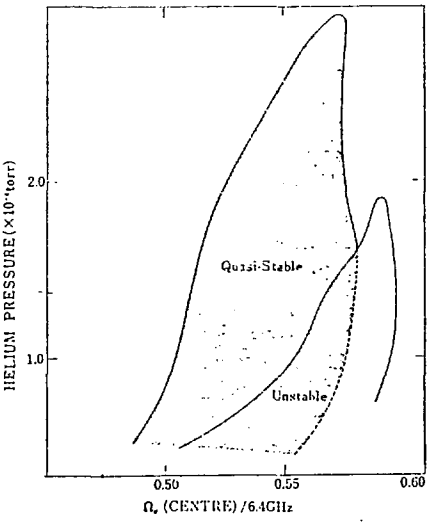

Fig.14. Region of the stable and unstable state. In the quasi-stable region, the instability can be triggered artificially.

Acknowledgement

The authors like to express appreciations to those who participated in the experiments of TPM mirror program in the past ten years for their collaboration, especially to Professor S. Tanaka of Kyoto University, Professor S. Aihara of University of Campinas, and Dr. H. Ikezi of Bell Laboratories.

REFERENCES

1. H. Ikegami, et al., Phys. Rev. Let. 19 (1967) 770.
2. R. A. Dandl, et al., "Electron-Cyclotron Heated 'Target' Plasma Experiment", in *Plasma Physics and Controlled Nuclear Fusion Research* (Proc. Int. Conf. Novosibirsk, 1968) Vol.2, IAEA, Vienna (1969) 435.
3. K. Uo, et al., "Behavior of Ohmically Heated Plasma in a Heliotron Magnetic Field" in *Plasma Physics and Controlled Nuclear Fusion Research* (Proc. Int. Conf. Novosibisrk, 1968) Vol.1, IAEA Vienna (1969) 217.
4. T. Uchida, et al., "Confinement of a Toroidal Theta-Pinch Plasma in a Periodic Caulked-Cusp Field" in *Plasma Physics and Controlled Nuclear Fusion Research* (Proc. Int. Conf. Madison, 1970) Vol.3, IAEA, Vienna (1971) 169.
5. V. G. Zykov, et al., Sov. Phys. Tech. Phys. 19 (1975) 1063.
6. R. A. Dandl, et al., "Plasma Confinement and Heating in the ELMO Bumpy Torus (EBT)" in *Plasma Physics and Controlled Nuclear Fusion Research* (Proc. Int. Conf. Tokyo, 1974) Vol.2, IAEA, Vienna (1975) 141.
7. T. Shoji et al., "Plasma Confinement in Nagoya Bumpy Torus" in *Proc. 9th European Conf. on Controlled Fusion and Plasma Physics, Oxford, 1979*, Vol.1 (1979) 2.
8. M. Fujiwara, et al., "Experimental Studies of Plasma Confinement in the Bumpy Torus" in *Plasma Physics and Controlled Nuclear Fusion Research* (Proc. Int. Conf. Brussels, 1980) IAEA-CN-38/BB-4.
9. M. C. Becker, et al., Nucl. Fusion: 1962 Supplement, Part 1, 345.
10. R. A. Dandl, et al., Nucl. Fusion 4 (1964) 344.
11. W. B. Ard, et al., Phys. Fluids 9 (1966) 1498.

12. W. B. Ard, et al., "Energetic Neutral Injection into an Electron-Cyclotron Plasma" in *Plasma Physics and Controlled Nuclear Fusion Research* (Proc. Int. Conf. Culham, 1965) Vol.2, IAEA, Vienna (1966) 153.

13. H. Ikegami, et al., Phys. Fluids 11 (1968) 1061.

14. H. Ikegami, et al., "Characteristics of Microinstabilities in a Hot-Electron Plasma", in *Plasma Physics and Controlled Nuclear Fusion Research* (Proc. Int. Conf. Novosibirsk, 1968) Vol.2, IAEA, Vienna (1969) 423.

15. H. Ikegami, et al., Nucl. Fusion 13 (1973) 351.

16. M. Fujiwara, et al., "The Ring Formation in Nagoya Bumpy Torus", *Proc. Workshop on EBT Ring Physics*, ORNL-CONF-791228 (1979) 123.

17. H. Ikegami, et al., Ann. Rev. IPP-Nagoya (April 1969 - March 1970) 29.